PRAMANA
—journal of
physics

© Printed in India

Vol. 49, No. 6,
December 1997
pp. 623–633

Measurement of excitation functions and mean projected recoil ranges of nuclei in ^{12}C-induced reactions on vanadium

M ISMAIL, R P SHARMA and M H RASHID
Variable Energy Cyclotron Centre, I/AF, Bidhan Nagar, Calcutta 700 064, India
Email: ismail@veccal.ernet.in

MS received 19 October 1996; revised 16 June 1997

Abstract. Excitation function and mean projected recoil ranges of nuclei produced in the ^{12}C-induced reactions on ^{51}V target were measured by conventional stacked foil and thick-target thick-recoil-catcher technique for bombarding energies $E \leq 84$ MeV for ^{12}C ion beam. The measured recoil ranges are converted to momentum transfer. Information on momentum transfer was used to get clues about some aspects of the interaction such as complete fusion which corresponds to full momentum transfer and incomplete fusion reaction mechanism. The measured excitation functions are compared with the calculation based on the statistical model which describes only equilibrium decay of the compound nucleus using the Cascade code and the geometry dependent hybrid model which describes equilibrium as well as pre-equilibrium decay of the compound nucleus using the Alice/91 code. The measured excitation functions and average ranges of the radioisotope products of the reactions ^{12}C on ^{51}V indicate that the three separate reaction mechanisms could be attributable to complete fusion of ^{12}C, incomplete fusion of ^{8}Be and incomplete fusion of ^{4}He respectively with the target. The ^{8}Be and ^{4}He are the break-up component of ^{12}C into ^{8}Be + ^{4}He. The predictions of the codes, especially the Cascade, generally agree with the measured cross-sections which could be attributed to complete fusion of ^{12}C with the target ^{51}V.

Keywords. ^{12}C-induced reactions on vanadium; stacked foil technique; isotope production; equilibrium decay; Cascade and Alice/91 codes.

PACS No. 25.60

1. Introduction

For many years now there has been a great interest to study the reaction mechanism in medium energy heavy-ion induced reactions. Most of the earlier studies have concentrated on the energy, angular momentum and charge distribution of the products emitted in heavy-ion reactions, while others are interested in multifragmentation which are intimately connected with that of complex or intermediate mass fragments. In recent years there has been considerable interest to study fusion and incomplete fusion (ICF) in heavy ion reactions at projectile energies in the range of 5–10 MeV/amu [1]. The motivation for this work was to use the ^{12}C ions and other ion beams such as ^{7}Li, ^{14}N and ^{16}O from BARC–TIFR Pelletron Accelerator Facility to study the fusion and incomplete fusion (ICF) reaction mechanism by measuring the cross-section and recoil ranges of

radioactive products which could be converted to linear momentum transfer to the compound nucleus.

In the case of fusion reaction the highly excited nuclear system decays by evaporating low energy nucleons and alpha particles at the equilibrium stage. While in the case of ICF reaction only a part of the projectile fuses with the target nucleus and the other part moves in beam direction with almost the same velocity as that of incident ion beam. The excitation function and mean projected recoil ranges of nuclei produced in the ^{12}C-induced reactions on ^{51}V target were measured by conventional stacked foil and thick target thick recoil catcher technique for bombarding energies $E \leq 84$ MeV ^{12}C ion beam. The work reported here also relates to the measurements of the recoil ranges of nuclei produced, to get experimental information about the momentum transfer associated with specific final nuclei. The linear momentum transfer characteristics of reactions supplement the energy partitioning characteristics of the reactions. The average linear momentum transfer characterizes the global features of the projectile target interaction and provides a convenient indication of the reaction mechanism. It will be largest for complete fusion reactions and reduced for direct (incomplete fusion), pre-equilibrium and break-up processes in which much of the incident momentum is carried away by the fast particles in the early stages of the reaction. Experiments have been performed at the BARC–TIFR (14-UD Pelletron) Medium Energy Heavy Ion Accelerator Facility at Bombay. Several techniques have been devised to measure the momentum of the recoil nuclei. Measurement of recoil velocity of the detected heavy products can be used to identify the fusion modes i.e. the complete fusion or incomplete fusion (ICF). Attempts to measure recoil velocity have been made in time of flight studies; however only the mass of the residue is identified and not its atomic number. If the heavy residue is a radio isotope, the original recoil velocities could be inferred from its range measurement in a stopping medium. This is a long established way of investigating heavy-ion reactions [2–4].

In the present work the linear momentum transfer characteristic in the ^{12}C-induced reactions on ^{51}V, was obtained employing the classical method of thick-target thick-catcher recoil range measurements [2–4]. Several excitation functions for the ^{12}C-induced reactions on ^{51}V measured by using the stacked foil technique are presented. The excitation functions of the radioactive products observed in reactions contain some information about the mechanism of the interaction of the ^{12}C-induced reactions on ^{51}V and we will be able to decipher some features of the partitioning of the incident energy into that carried away by outgoing fast particles at the pre-equilibrium stage (in contrast to evaporation), and that left as nuclear excitation by using the code Alice/91 [5]. In this work calculations in the framework of the equilibrium statistical model using the codes Cascade [6] and pre-equilibrium model using the code Alice/91 [5] were performed and the results are compared with experimental excitation functions. Various reaction mechanisms, supported by recoil range measurements, are indicated as contributing to the production of the radioactive nuclei.

2. Experimental procedure

Excitation functions and mean projected recoil ranges of the nuclei produced in the ^{12}C-induced reactions on ^{51}V were measured using the absolute yields of characteristic γ-rays

pertaining to the decay of each radioactive residual nuclei by off-line γ-ray measurements. The targets were obtained by rolling vanadium foils using the rolling machine at TIFR, Bombay. The thickness of the targets for excitation function measurements was about $\cong 2.0\,\mu m$ whereas for the range measurements the thickness was about $\cong 8.0\,\mu m$. The stacks were formed by placing alternatively 4.34 μm aluminium foils as degraders of ^{12}C energy over the targets. Then the stacks were irradiated in a chamber specially constructed for this purpose by BARC, Bombay and having the facility to suppress electron in the Faraday cup by applying negative bias. The beam spot on the targets was limited to 5.0 mm diameter by using a stainless steel collimator in front of the targets. There were 13 targets in the stack for the excitation function measurement and 3 to 4 targets in the stack for recoil range measurements. The stacks were exposed to the analysed beam from the 14UD tandem pelletron accelerator facility at TIFR, Bombay. The beam current on the targets was kept below 200 enA. The total ^{12}C-beam was collected and measured using a calibrated current integrater.

The average thickness of the target and degrader foils was determined by weighing. Each foil was cut out into a square shape and pasted on an annular aluminium holder having 21.0 mm as the outer diameter and 15 mm as the inner diameter.

The efficiency calibrations of the detector were done with a standard ^{152}Eu radioactive source. The efficiency of the detector was interpolated to the required energy value from the measured efficiency curve. However to improve the interpolation, the efficiency curve was fitted to a function of the form

$$\varepsilon(E_\gamma) = \sum_{i=1,4} A_i * (E_\gamma)^{i-1} + B_1 \exp(-B_2 * E_\gamma) \tag{1}$$

by a non-linear least square method (for details see ref. [7]) where A_i and B_i are constants to be determined by least-square fit and E_γ is the γ-ray energy. The fit improves the accuracy of interpolation considerably.

The mean beam energy at half thickness in each foil of a stacked foil assembly was calculated from energy degradation of the initial beam energy using the coefficients obtained from fitting the stopping power data for different materials. The α-stopping power tables of Williamson *et al* [8] were used for fitting. Then the stopping power S for a given combination of stopping medium and heavy-ion beam and velocity is calculated by means of the well-known scaling law

$$S/(\gamma Z_1)^2 = S_{\text{ref}}/Z_{\text{ref}}^2 \tag{2}$$

in which (γZ_1) is the heavy-ion effective charge (Z_1 being its atomic number) and S_{ref} is the stopping power of the same medium for a reference ion (α-ion) of the same velocity and of effective charge Z_{ref}. The tabulation is then generated based on the arguments of the effective charge parameter γ (Z_1, E/A, Z_2) given in [9]. The stopping power generated in this way is very similar to that generated by the code TRIM.

The production cross-sections were determined using the absolute yields of characteristic γ-rays belonging to each final nucleus. The γ-rays emitted by the irradiated targets and their associated catcher foils were detected with a HPGe detector available at TIFR, Mumbai as well as VECC, Calcutta. In most of the cases the γ-rays used in the yield determination (listed in table 1) stood out very prominently in the spectra and did

Table 1. Half-lives, γ-energies and branching ratios of the γ-decays and Q-values for C-induced reactions on V.

Nuclide	Half-lives	E_γ (keV)	I_γ (abs)	Reaction	Q-values (keV)
^{24}Na	14.96 h	1368.6	1.0	^{27}Al(C, $2\alpha 4p3n$)^{24}Na	−66997.4
				^{27}Al(C, $3\alpha 2pn$)^{24}Na	−38701.5
				^{27}Al(C, C $2pn$)^{24}Na	−31426.7
				^{51}V(C,^{37} Clpn)^{24}Na	−27378.9
^{58}Co	70.76 d	810.80	0.994	^{51}V(C, $2p3n$)^{58}Co	−31147.6
				^{51}V(C, αn)^{58}Co	−2851.7
^{57}Co	271.7 d	122.10	0.856	^{51}V(C, $2p4n$)^{57}Co	−39720.7
				^{51}V(C, $\alpha 2n$)^{57}Co	−11424.9
^{56}Co	78.76 d	846.80	0.999	^{51}V(C, $2p5n$)^{56}Co	−51096.6
				^{51}V(C, $\alpha 3n$)^{56}Co	−22800.7
^{54}Mn	312.2 d	835.00	1.000	^{51}V(C, $4p5n$)^{54}Mn	−66158.7
				^{51}V(C, $\alpha p3n$)^{54}Mn	−37862.8
				^{51}V(C, $2\alpha n$)^{54}Mn	−9566.9

not pose any identification problem. The γ-ray spectra from the HPGe spectrometers were recorded on 3.5″ diskettes by using PC-based data acquisition system. The spectra were later analysed by personal and SUPER-32 computers. The methods of analysis of the γ-ray spectra and the efficiency calibrations of the detector were the same as reported in ref. [10, 7].

The nuclear data necessary for the evaluation of the cross sections are presented in table 1. The half-lives of the radioactive atoms are taken from the chart of nuclides, the γ-rays energies and branching ratios are taken from the table of isotopes [12]. In table 1 only those γ-rays are listed which were chosen for the calculation of the cross-sections. Q-values were calculated using the atomic mass table of Wapstra and Audi [13].

2.1 *Recoil range measurements*

Several techniques have been devised to measure the momentum of the recoiling nuclei. In the present work the linear momentum transfer characteristics in the ^{12}C-induced reactions on ^{51}V, were obtained employing the classical method of thick-target thick-catcher recoil range measurement technique ([2], [3] and [4]). If the target and catcher foils are perpendicular to the beam axis and the target thickness is larger than the maximum observable recoil range and let x be the fraction recoiling forward, then $(1-x)$ is the corresponding fraction recoiling backwards, N the number of residual nuclei produced per unit length of the target thickness, R_F and R_B the forward and backward ranges, T the target thickness and A_F, A_B and A_T the activities induced in the forward and backward catchers and in the target. Then it easily follows that

$$A_F = xNR_F; \quad A_B = (1-x)NR_B; \quad A_T = NT - A_F - A_B. \tag{3a-c}$$

Hence

$$A_F/(A_F + A_T) = xR_F/[T - R_B(1 - x)]. \tag{3d}$$

Since x is close to unity, one can neglect the last term in the denominator $(1 - x) \cong 0$ which is small in comparison with the target thickness and then one obtains

$$R_F = T \cdot A_F/(A_F + A_T). \tag{4}$$

This relation has been used in this work to measure the mean forward range in the ^{12}C-induced reactions on ^{51}V.

In order to obtain information about the linear momentum of the recoil products, their ranges were converted to velocities parallel to the beam direction (V_p) with the help of range-energy relation $d\varepsilon/d\rho$ given by Lindhard, Scharff and Schiott theory [14]. The stopping power $d\varepsilon/d\rho$ is the sum of two terms

$$d\varepsilon/d\rho = (d\varepsilon/d\rho)_e + (d\varepsilon/d\rho)_n. \tag{5}$$

For the electronic energy loss, the expression $(d\varepsilon/d\rho)_e = k\sqrt{\varepsilon}$ given by Lindhard and Scharff [15] is used. For the energy loss due to nuclear collision the expression $(d\varepsilon/d\rho)_n = -c\log\{\varepsilon^\alpha/a + b/\varepsilon^\beta\}$ with $c = 0.2$, $\alpha = 1.215$, $a = 70.0$, $b = 0.002$ and

Table 2. Experimental and calculated ranges for the products in $^{51}V + ^{12}C$ reaction.

$E \pm \Delta E$ (MeV)	Recoil energy (MeV)	Range (μm) and recoil energy of the products				
		^{58}Co	^{57}Co	^{56}Co	^{56}Mn	^{54}Mn
80.8 ± 3.2	15.4	3.3 (3.8 ± 0.3) 14.2*	3.3 (2.5 ± 0.2) 13.9*	3.2 (2.6 ± 0.2) 13.7*	3.4 (2.7 ± 0.2) 13.7*	3.3 (1.7 ± 0.1) 13.2*
72.1 ± 3.5	13.7	3.1 (3.0 ± 0.2) 12.6*	3.0 (3.0 ± 0.2) 12.4*	2.93 (2.5 ± 0.2) 12.2*	3.2 (2.3 ± 0.2) 12.2*	3.0 (2.1 ± 0.2) 11.8*
66.3 ± 3.7	12.6	2.9 (3.4 ± 0.3) 11.6*	2.8 (3.1 ± 0.3) 11.4*	2.8 (2.3 ± 0.2) 11.2*	3.0 (2.1 ± 0.2) 11.2*	2.9 (2.3 ± 0.2) 10.8
62.7 ± 3.8	11.9	2.7 (2.1 ± 0.2) 11.0*	2.7 (2.7 ± 0.2) 10.8*	2.7 (2.8 ± 0.2) 10.6*	2.8 (1.4 ± 0.1) 10.6*	2.7 (1.8 ± 0.1) 10.2*
$56.2 + 4.0$	10.7	2.5 (3.3 ± 0.3) 9.9*	2.5 (2.6 ± 0.2) 9.7*	2.4 (1.4 ± 0.1) 9.5*	2.6 (0.8 ± 0.1) 9.5*	2.5 (1.7 ± 0.1) 9.2*
44.9 ± 4.7	8.6	2.1 (4.0 ± 0.3) 7.9*	2.1 (1.8 ± 0.1) 7.7*	2.0 7.6*	2.2 7.6*	2.1 (0.7 ± 0.1) 7.3*

The measured recoil ranges are within ( ) and the corresponding recoil energies are marked with (*). The calculated ranges are having $\cong$ 15% error due to errors in the stopping power parameter. See eq. (5).

$\beta = 0.815$. In the recoil range limits which are relevant to the present work, the ranges are almost exactly proportional to the recoil velocity as shown above as well as in Northcliff and Schilling [16, 17]. It was shown in [18] that under these conditions, and with the assumption of an isotropic distribution of the evaporation vector, the evaporation contribution to the thick target recoil ranges may be neglected to the first order. The correction to (V_p) arising from the angular distribution of the recoils $\langle \cos\phi \rangle$, due to atomic collisions, was calculated by the expression derived by Blaugrund [19], where ϕ is the average scattering angle due to nuclear collision. The constants used in the expressions for $(d\varepsilon/d\rho)_e$ and $(d\varepsilon/d\rho)_n$ are having $\cong 15\%$ errors, thereby introducing $\cong 15\%$ errors in the calculated range values also.

The technique for the range measurement mentioned above assumes uniform production cross-section for the nuclei throughout the target width in energy units so that the activities A_F, A_B and A_T are exactly proportional to forward range, backward range and total target thickness. In the present work range measurements for the ^{12}C-induced reactions on ^{51}V target are shown in table 2. The thickness of ^{51}V targets correspond to $\cong 6.4$ MeV in energy units for 84 MeV ^{12}C-ion and $\cong 09.5$ MeV for the 44 MeV ^{12}C-ion. Therefore, in the present case (^{51}V target) the cross-section at the two edges differ appreciably compared to the average cross-section over the target thickness. If the bombarding energy is at the rising part of the excitation function as seen from the high energy side then the range extracted by this method will be larger than the actual range whereas if the bombarding energy is at the declining part of the excitation function then the opposite will be true i.e. the extracted range will be smaller than the actual range. This is the reason why some of the extracted ranges are higher and others smaller than the calculated ranges. However the extracted ranges help in some cases to distinguish between compound nucleus by fusion reaction and incomplete fusion reaction including direct reaction mechanisms.

2.2 *Cross-section determination*

The number of observed decays Z per unit time is related to the total number of decays Z_0 per unit time by

$$Z_0 = Z/[\varepsilon(E_\gamma) * I_\gamma(\text{abs})], \tag{6}$$

where $\varepsilon(E_\gamma)$ is the detector efficiency and $I_\gamma(\text{abs})$ is the absolute γ-ray abundance per decay. The total number of decays, Z_0, is related to total reaction yield R for simple decays (simple decays correspond to direct production of radio isotopes by the nuclear reactions and we have used only such decays in all the measurements reported here) by the relation

$$R = Z_0 \cdot \exp(\lambda T_2)/[(1 - \exp(-\lambda T)) \cdot (1 - \exp(-\lambda T_1))/\lambda T_1], \tag{7}$$

where λ is the decay constant, T_1 the irradiation time and T_2 the cooling time after the end of irradiation and the beginning of the measurement and T is the counting time. R is related to the cross-section σ by the relation

$$\sigma = R/[(N_A \cdot \delta x) \cdot \mathcal{I}], \tag{8}$$

Table 3. Experimental cross-section for ^{12}C-induced reaction with ^{51}V.

Energy $\pm\Delta E$ (MeV)	Cross-sections for the products (mb)				
	Co-57	Co-58	Co-56	Mn-54	Na-24
83.2	48.4	122.0	23.3	79.3	13.3
±0.8	±3.9	±9.8	±1.9	±6.3	±1.1
79.7	64.8	185.9	44.4	109.1	11.7
±0.8	±5.2	±14.9	±3.6	±8.7	±0.9
76.0	68.4	170.4	47.8	119.6	10.5
±0.9	±5.5	±13.6	±3.8	±9.6	±0.8
72.3	73.1	138.4	51.3	131.8	8.0
±0.9	±5.8	±11.1	±4.1	±10.5	±0.6
68.5	102.2	114.1	60.7	155.1	6.0
±0.9	±8.2	±9.1	±4.9	±12.4	±0.5
64.4	132.7	72.9	52.9	163.7	4.5
±1.0	±10.6	±5.8	±4.2	±13.1	±0.4
60.2	163.0	48.6	37.7	154.4	2.9
±1.0	±13.0	±3.9	±3.0	±12.4	±0.2
55.7	200.7	53.5	22.5	135.9	2.3
±1.1	±16.1	±4.3	±1.8	±10.9	±0.2
51.1	180.9	67.3	7.7	79.3	1.8
±1.1	±14.5	±5.4	±0.6	±6.3	±0.1
46.0	166.8	93.4	0.0	36.9	2.5
±1.2	±13.3	±7.5		±3.0	±0.2
40.5	94.9	90.0	0.0	12.3	1.7
±1.3	±7.6	±7.2		±1.0	±0.1
34.4	25.4	52.2	0.0	0.0	3.1
±1.5	±2.0	±4.2			±0.2

where N_A is the number of atoms/cm^3 of the target material, δx is the thickness of the foil (in cm) and $\mathcal{I}$ is the total number of incident particles during irradiation (calculated from total charge measured by current integrator).

3. Experimental results

In table 3 and figures 1a to 1d our experimental results for the production of ^{54}Mn, ^{56}Co, ^{57}Co, ^{58}Co and ^{24}Na radio-nuclides via ^{12}C-induced reactions on ^{51}V are summarized. The radio-isotope ^{24}Na could also be produced by ^{12}C induced reaction on ^{27}Al which is used as catcher foils in the stacks. The possible Q-values are listed in table 1. The uncertainty given for the energy values includes those of target thickness and beam energy resolution (±5.0 keV) only. The solid lines and the dashed lines are respectively the Cascade code [6] and Alice/91 [5] fits. In table 3 the experimental cross-sections for the reaction $^{12}C + {}^{51}V$ are presented respectively along with absolute errors of $\cong$ 8%. The absolute error consists of uncertainties due to target foil thickness (±2%), the beam current integration (±2%), the detector efficiency (±5%) and the analysis of the γ-ray spectra (statistical uncertainty) generally ($\leq$ 2%). The uncertainties caused by the large size of the irradiation area and the non-uniformities of the target contribute about 5% to

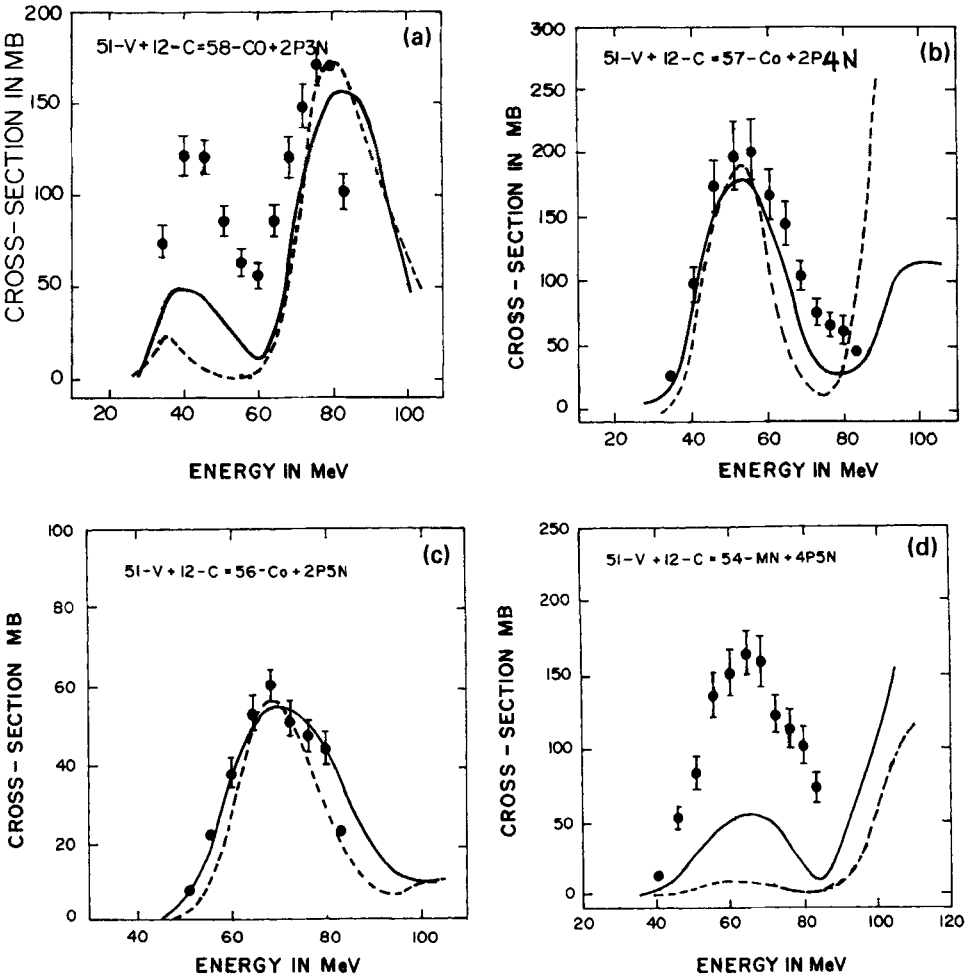

Figure 1. The total residual production cross-section in mb for the reaction (**a**) ^{51}V (^{12}C, $2p3n$) ^{58}Co (•), (**b**) ^{51}V (^{12}C, $2p4n$) ^{57}Co (•), (**c**) ^{51}V (^{12}C, $2p5n$) ^{56}Co (•) and (**d**) ^{51}V (^{12}C, $4p5n$) ^{54}Mn (•) are plotted as a function of ^{12}C-particle bombarding energy. Solid lines are the Cascade model calculation and dashed lines are Alice/91 calculation with $N_0 = 12$, $N_n = 6$, $N_p = 6$ and $N_h = 0$, normalized to experimental values at the maximum cross-section point with normalization constant $N = 1.00$ for all the solid line curve and for the dashed line curves (**a**) $N = 0.5$, (**b**) $N = 1.0$, (**c**) $N = 0.3$ and (**d**) $N = 1.0$.

the average error of the cross-section. However, the above mentioned average error values do not include the uncertainties of the nuclear data used in the analysis.

4. Comparison with theoretical predictions

A rigorous theory of nuclear reaction for which calculations can be performed to describe mass, angular and energy distribution data from intermediate energy collision with

complex particle is presently not available. A simpler compound statistical model is generally applicable below 7 MeV/nucleon owing to very low probability for pre-equilibrium and direct reaction processes [20]. However, the energy range of present work is also ≤ 7 MeV/nucleon only. Hence our discussion will be based mostly on compound statistical models. It is well-known that the compound statistical model gives a correct overall description of the excitation functions and particle energy spectra in nuclear reactions at medium energies. However, the calculations fail to account for all details such as the exact position of the maximum or the slope of the ascending and descending part of the excitation functions. We have investigated the nuclear mechanism of the nuclear reaction $^{12}C + ^{12}V$ by using the two computer codes Cascade [6] and Alice/91 [5]. The Cascade code is based on the assumption that the projectile and target form a compound nucleus in statistical equilibrium and Hauser–Feshbach formula together with the statistical nuclear model are applied in order to calculate the intensities of the various decay chains and thus the excitation functions of the reactions. The Alice/91 code describes the process of equilibrium evaporation of particles and γ-rays in terms of the Weisskopf and Ewing model [21] and pre-equilibrium reaction mechanism according to the hybrid and geometry dependent hybrid model. The high energy part of the excitation functions are dominated by pre-equilibrium reaction mechanism whereas the low energy parts are dominated by evaporation with its characteristic peak as seen in [7, 10]. Besides evaporation of neutrons and protons, clusters such as deuteron and α-particles can be considered. The nuclear masses were taken from Wapstra and Audi [13] mass table if available, otherwise calculated from the Mayers and Swiatecki mass formula [22], liquid drop masses with pairing. The inverse cross-sections were calculated using the optical model subroutine of Alice/91 [5], where the optical model parameters were those of Becchetti and Greenlees [23]. In the present work our excitation functions are calculated on the basis of (i) statistical model which describes only equilibrium decay using the code Cascade [6] and (ii) geometry dependent hybrid model [24] using the program Alice/91 [5] on the super-32 computer at our centre. In figures 1a to 1d, the filled circles are measured cross-sections. The theoretical values shown in the figures 1a to 1d are multiplied by a factor so as to match the experimental data at the maximum cross-section point. The multiplying factors are given in the figure captions. The multiplying factors also indicate the quality of fit between experimental and theoretical values. The dashed curves and solid curves are the calculated cross-section based on the codes Alice/91 and Cascade respectively. Figures 1a to 1c show that the excitation functions for the $2pxn$ or αxn channels are predicted reasonably well by Cascade code whereas Alice/91 code fits only ^{56}Co excitation function fairly well. However there is one exception i.e. the first peak in the excitation function for the production of ^{58}Co which the codes underpredict. This is mostly due to αn channel as seen in the excitation function for the reaction $^{59}\mathrm{Co}(\alpha, \alpha n)^{58}\mathrm{Co}$ (see ref. [11]). Figure 1d shows the excitation function for the $2\alpha n$ or $4p5n$ channels for the production of ^{54}Mn. Both the codes underpredict the production cross-sections. These possibly indicate that these radio-isotopes ^{58}Co and ^{54}Mn are not only produced by α-evaporation but also by another mechanism possibly by break-up of ^{12}C into α and ^{8}Be. Then the fusion of ^{8}Be and evaporation of a neutron to produce ^{58}Co and the fusion of α and evaporation of a neutron to produce ^{54}Mn radio isotopes. The measured average ranges also support the incomplete fusion reaction mechanism. In Cascade and Alice/91 codes evaporations of

only n, p and α particles are being taken into account. That is why they underpredict the incomplete fusion of ^{8}Be and ^{4}He with the target ^{51}V. However, the predictions of these codes, especially the Cascade, generally agree with the measured cross-sections which could be attributed to complete fusion of ^{12}C with the target ^{51}V.

5. Conclusion

A consistent set of 4 excitation functions has been measured for ^{12}C-induced reactions on ^{51}V target. The measured excitation functions and average ranges of the radioisotope products of the reactions ^{12}C on ^{51}V give some indication that the three separate reaction mechanisms which could be attributed to complete fusion of ^{12}C, incomplete fusion of ^{8}Be and incomplete fusion of ^{4}He respectively with the target. The ^{8}Be and ^{4}He are the break-up component of ^{12}C into ^{8}Be$+^{4}$He. It can be seen that the predictions of the codes, especially the Cascade, generally agree with the measured cross-sections which could be attributed to complete fusion of ^{12}C with the target ^{51}V.

Acknowledgements

The authors thank the staff of Pelletron at TIFR for help. They also thank Mr P P Burte for technical help and Dr M Blann for supplying the Alice/91 code.

References

[1] B S Tomar, A Goswami, A V R Reddy, S K Das, P P Burte, S B Manohar and Satyaprakash, *Z. Phys.* **A343**, 223 (1992)
B S Tomar, A Goswami, A V R Reddy, S K Das, P P Burte and S B Manohar, *Phys. Rev.* **C49**, 941 (1994)
[2] N Sugarman, M Campos and K Wielgoz, *Phys. Rev.* **101**, 388 (1956)
[3] J M Alexander, in *Nuclear Chemistry* edited by L Yaffe (Academic, New York, 1968) vol. 1, p. 273
[4] J M Alexander and G N Simonoff, *Phys. Rev.* **B133**, 93 (1964)
[5] M Blann, Alice/1991 – *A Evaporation Code* (Lawrence Livermore National Lab, University of California, Livermore UCID-20169, 1985)
[6] F Puhlhofer, *Nucl. Phys.* **A280**, 267 (1977)
[7] M Ismail, *Phys. Rev.* **C41**, 87 (1990)
[8] C F Williamson, J P Boujot and J Picard, CEA-R 3042 (1966)
[9] F Hubert, R Bimbot and H Gavin, *Atomic Data Nucl. Data Tables* **46**, 1 (1990)
[10] M Ismail and A S Divatia, *Pramana – J. Phys.* **30**, 193 (1988)
M Ismail, *Pramana – J. Phys.* **32**, 605 (1989)
[11] M Ismail, *Pramana – J. Phys.* **40**, 227 (1993)
R Michel and G Brinkmann, *Nucl. Phys.* **A338**, 167 (1980)
[12] C M Lederer and V S Shirley, *Table of Isotopes*, 7th edition (New York, John Wiley, 1978)
[13] A H Wapstra and G Audi, *Nucl. Phys.* **A432**, 1 (1985)
[14] J Lindhard, M Scharff and H E Schiott, *Matt. Fys. Medd. Dan. Vid. Selsk.* **33**, 14 (1963)
[15] J Lindhard and M Scharff, *Phys. Rev.* **124**, 128 (1961)
[16] L C Northcliffe, *Annu. Rev. Nucl. Sci.* **13**, 67 (1963)
[17] L C Northcliffe and R F Schilling, *Nucl. Data Tables* **A7**, 233 (1970)
[18] L Winsberg and J M Alexander, *Phys. Rev.* **121**, 518 (1961)
[19] A E Blaugrund, *Nucl. Phys.* **88**, 501 (1966)

[20] R Birkland, L E Tubbs, J R Huizenga, J N De and D Sperber, *Phys. Rep.* **56**, 108 (1979)
[21] V F Weisskopf and D H Ewing, *Phys. Rev.* **57**, 472 (1940)
[22] W D Myers and W J Swiatecki, *Nucl. Phys.* **81**, 1 (1966)
W D Myers and W J Swiatecki, *Ark. Fys.* **36**, 343 (1967)
[23] F D Becchetti and F D Greenlees, *Phys. Rev.* **182**, 1190 (1969)
[24] M Blann, *Phys. Rev. Lett.* **27**, 337 (1971)
M Blann, *Phys. Rev. Lett.* **28**, 757 (1972)